Proceedings of 2007 IDETC/CIE
2007 ASME International Design Engineering Technical Conferences &
and Computers and Information in Engineering Conferences
September 4-7, 2007, Las Vegas, USA

DETC2007-34409

DEVELOPMENT OF EXTENDED WHEELCHAIR OPERATION OBSERVER TO ESTIMATE PRECISE TWO-DIMENSIONAL TILT INFORMATION

Sehoon Oh

Institute of Industrial Science
University of Tokyo
4-6-1, Komaba, Meguro, Tokyo, 153-8505 Japan
Email: sehoon@horilab.iis.u-tokyo.ac.jp

Yoichi Hori

Institute of Industrial Science
University of Tokyo
4-6-1, Komaba, Meguro, Tokyo, 153-8505 Japan
Email: hori@iis.u-tokyo.ac.jp

ABSTRACT

An operation states observer for a wheelchair system is extended to three dimensions in this paper. This new observer incorporates a three-axis accelerometer allowing a user to estimate more precise information on terrain condition.

To design this observer, first, a model dynamics illustrating the two-dimensional relationship between the gravity and the motion of a wheelchair on a slope is derived. Experimental results verify our derivation of equations. Then, the dynamics is simplified and used in the design of the extended observer. Since the dynamics itself and the output of that have nonlinear characteristics, the extended kalman filter design algorithm is employed. By simulation, the stability and effectiveness of the application is verified.

Key Words : *wheelchair, operation states observer, extended kalman filter, two-dimensional effect of the gravity, human friendly motion control, three-axis accelerometer*

1 Introduction

Recently, various kinds of power wheelchairs have been developed and suggested [1], [2]. In addition to the electric-powered wheelchairs which are now quite broadly used, pushrim-activated, power-assisted wheelchair (PAPAW) [2] has been focused as a new mobility assistance. In all these power assisted wheelchair needs proper control algorithm and that control algorithm can be improved if we can get precise information on terrain condition where the wheelchair is located. We have suggested an operation states observer of a wheelchair for this power assist control and it provided important operational conditions in [3]. This paper extends the states that the operation states observer can estimate into three dimensions.

1.1 Operation States Observer in a Power-assisted Wheelchair

In [3], operation states described in Figure 1 (a) are accurately estimated using the kalman filter algorithm. v is driving speed of a wheelchair in the longitudinal direction, φ is inclination angle which means the leaning angle of the wheelchair frame from the horizon. These variables are necessary for the power assist control of a wheelchair [3] but cannot be accurately measured by sensors. Figure 1 (b) is the measurements of the

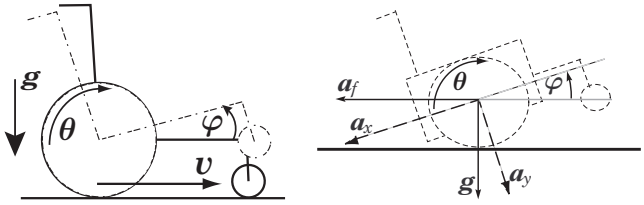

(a) states of wheelchair (b) measurements of sensors

Figure 1. Operation States and Measured Information

wheelchair. θ is the rotated angle of a wheel, a_x, a_y are the output of an accelerometer, and $\dot{\varphi}$ is the output of a gyroscope.

Since this previous observer [3] uses two-dimensional accelerometer, any information on the lateral direction cannot be measured. The gravity acting in the lateral direction, illustrated in Figure 2 will not be estimated in this observer.

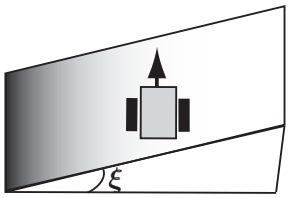

Figure 2. Gravity Acting Laterally on a Wheelchair

This gravity in the lateral direction, however, interferes with the heading direction of a wheelchair and is quite important information in assisting a wheelchair. This is the reason why this paper suggests an extended operation states observer.

1.2 Extension of Conventional Operation States Observer

If the angle ξ of the slope is obtainable, it must improve the control of a wheelchair. For this reason, we design a novel states observer to get information of the angle ξ.

Figure 3 illustrates the angles we will estimate by a novel observer design: the pitch angle of a wheelchair (φ) with regarding to its heading direction, the heading angle (α) with regard to the horizon and the slope angle (ξ) of a hill.

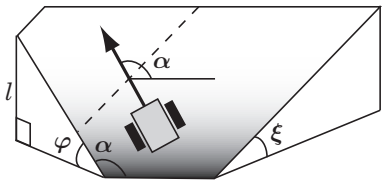

Figure 3. Angles Necessary for Safe Operation on a Slope

If we can distinguish these angles correctly from the measured values, the control of a wheelchair on a slope will be more safe and easy to operate by a user. For example, accurate values of these angles enable a controller to drive a wheelchair straightly in the face of the lateral gravity.

2 Describtion of Three-dimensional Operation State

In order to design a states observer, the relationship of operation states, especially the angles to be estimated should be analyzed at first.

2.1 Derivation of Output Equations Produced by Three Sensors

Three kinds of sensors are utilized in this system: one 3-axis accelerometer, two encoders on both wheels and one gyroscope which measures the pitch angle around the axis of wheels. These sensors provide φ, α, ξ in Figure 3 and the moving velocity *v* in Figure 1 (a).

In order to design an observer using these sensor outputs, the relationship between these outputs and state variables should be clarified. At first, output equations which tell how the state variables appear in sensor outputs are derived here.

Figure 3 shows the relationship between the pitch angle φ and the yaw or heading angle α of a wheelchair on a slope of ξ. This relationship will be described as Equation (1).

$$\sin\varphi = \sin\alpha\sin\xi \tag{1}$$

This equation reveals the output equation of the gyroscope which measures the angular velocity of φ. The equation is given as Equation (3).

$$\varphi = \sin^{-1}(\sin\alpha\sin\xi) \simeq \sin\alpha\sin\xi \tag{2}$$

$$\dot{\varphi} \simeq \dot{\alpha}\cos\alpha\sin\xi + \dot{\xi}\sin\alpha\cos\xi \tag{3}$$

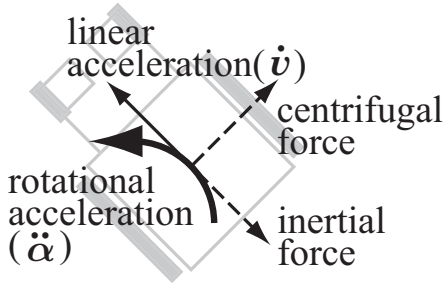

Figure 4. Decomposition of the Force Measured by an Accelerometer

Accelerometer measures the linear acceleration of the wheelchair including the gravity vector. In addition to the heading acceleration in the linear direction, yaw acceleration is also

measured by a three-axis acceleration. Equation (4) to (6) describe the output equations of a 3-axis accelerometer.

$$a_x = g\sin\xi\sin\alpha + \dot{v} + f_{\text{rotation}_x} \tag{4}$$
$$a_y = g\sin\xi\cos\alpha + v\dot{\alpha} + f_{\text{rotation}_y} \tag{5}$$
$$a_z = g\cos\xi, \tag{6}$$

where v illustrates the velocity of a wheelchair in its heading angle. The directions of x, y, z axes are illustrated in Figure 5.

The first term of each equation shows the gravity vector of which direction is determined by the condition α, ξ of a hill the wheelchair is located. The second terms represent the inertial force in Equation (4) and the centrifugal force in Equation (5). These are the forces manifested on the center of mass.

Meanwhile, $f_{\text{rotation}_{x,y}}$ are the forces caused by the fact that the accelerometer is not located in the center of mass of the wheelchair. Rotational motion around the center of mass produces additional acceleration measurements in the accelerometer. Figure 5 (a) shows the location of the accelerometer in a wheelchair. Since it is Δ_x, Δ_y off the center, additional inertial and centrifugal forces are applied to the accelerometer described in Equation (7) and (8).

$$f_{\text{rotation}_x} = \ddot{\alpha}\Delta_x + m\dot{\alpha}^2\Delta_y \tag{7}$$
$$f_{\text{rotation}_y} = -\ddot{\alpha}\Delta_y + m\dot{\alpha}^2\Delta_x \tag{8}$$

First terms are the output of the inertial force and second terms are the output of the centrifugal force. Notice that in this analysis of acceleration output, the center of gravity is assumed to be fixed so that Δ_x and Δ_y are dealt as known variables.

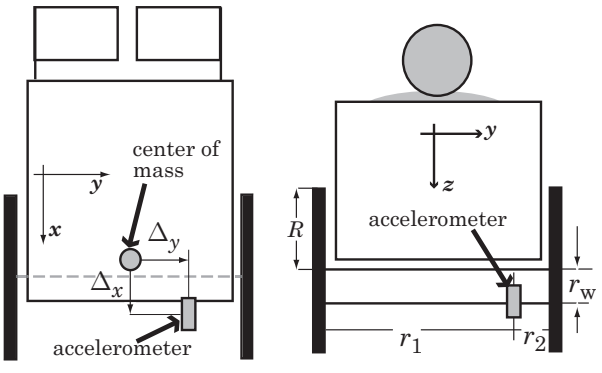

(a) Top view (b) Rear view

Figure 5. Location of an Accelerometer in a Wheelchair

If the slip between the wheels and the ground is ignored, the rotated angles of two wheels which are represented as θ_l, θ_r here, can be associated with the measured acceleration. v at the location of the accelerometer is identified with Equation (9) using θ_l, θ_r.

$$v = \frac{1}{2}(R\dot{\theta}_r + R\dot{\theta}_l), \tag{9}$$

where r_1, r_2, R means the lengths and distances illustrated in Figure 5. Also the heading angle α in Equation (5) can be derived from θ_l and θ_r as Equation (10) assuming no slip.

$$\alpha = \frac{R}{r_1 + r_2}(\theta_r - \theta_l) \tag{10}$$

Finally we obtain 6 output equations of all sensors, which contain the values of φ, α, ξ we want to estimate. The equations are re-described in Table 1.

Table 1. Output Equations

Gyroscope	$\dot{\varphi} = \dot{\alpha}\cos\alpha\sin\xi + \dot{\xi}\sin\alpha\cos\xi$
Accelerometer	$a_x = g\sin\xi\sin\alpha + \dot{v} + m\dot{\alpha}^2\Delta_y$
	$a_y = g\sin\xi\cos\alpha + v\dot{\alpha} - \ddot{\alpha}\Delta_y$
	$a_z = g\cos\xi$
Encoder	$v = \frac{1}{2}(R\dot{\theta}_r + R\dot{\theta}_l)$
	$\alpha = \frac{R}{r_1+r_2}(\theta_r - \theta_l)$

While the equation of a_x is straightforward, the equation of a_y is somewhat complicated. In order to verify that equation, three kinds of experiments are performed: 1) wheelchair rotates its heading angle without moving forward, 2) it turns right, 3) it goes forward and moves backward turning left.

In Figure 6, a_y described as a thick blue line represents the lateral acceleration measured by the accelerometer, while the thick blue line represents a_y calculated based on Equation (5) with the value of v and α from the encoder output. Two values are identified with each other, proving the correctness of Equation (5).

2.2 Derivation of Three-dimensional Dynamics

In order to build an states observer, a model of wheelchair dynamics is required; especially a model that describes how external force or the gravity affects on the motion of a wheelchair in the lateral direction. Dynamics of a wheelchair has many common points with that of a mobile robot. Some researches have modeled this dynamics [4], [5]. They focus on the coordinate

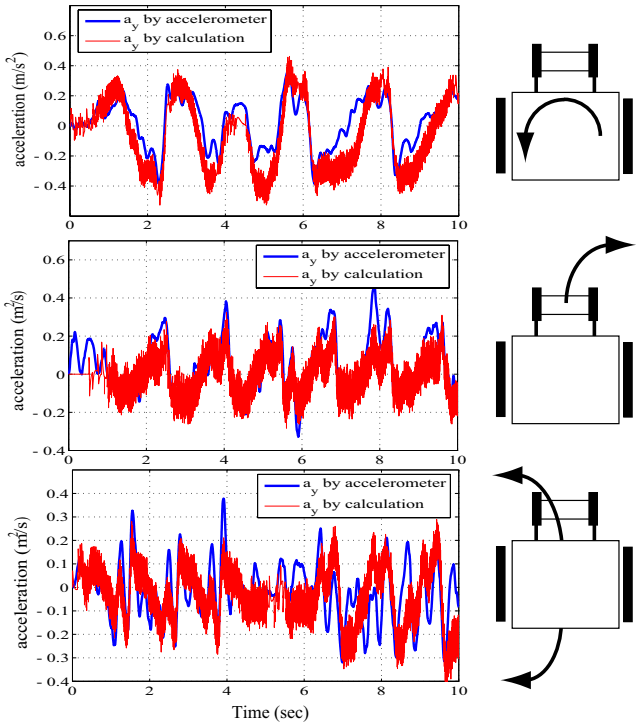

Figure 6. Comparison of Lateral Acceleration

conversion and the effect of rolling resistance, but the effect of the gravity in the lateral direction is not made clear in their modeling. This relationship will be clarified in this paper using the concept of the slip angle.

Since the lateral disturbance affects on the lateral motion of the wheelchair through the tires, the model should include the cornering force of the tires. This point is quite similar with the analysis on the dynamics of four-wheel vehicle. For this similarity, we adopt the dynamics modeling of vehicle dynamics not that of mobile robots to explain the lateral motion of a wheelchair.

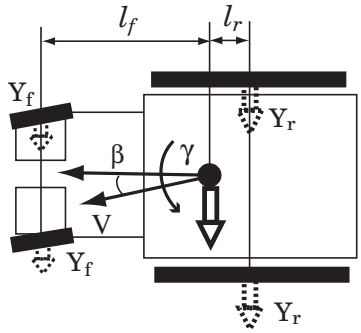

Figure 7. Lateral Motion of a Wheelchair

Figure 7 shows the relationship between the direction of moving velocity and heading direction. The difference is called as β or the slip angle in the vehicle engineering. When the gravity acts on the wheelchair in the lateral direction, that lateral force brings about the slip angle causing tire to produce cornering force. Finally the gravity results in the change of the heading angle. This relationship between the dynamics of β and the yaw rate γ is described in Equation (11) and (12).

$$mV\left(\frac{d\beta}{dt}+\gamma\right) = Y_f(\beta_f,\gamma)+Y_r(\beta_r,\gamma)+g_{\text{lat}} \tag{11}$$

$$I\frac{d\gamma}{dt} = l_f Y_f(\beta_f,\gamma)-l_r Y_r(\beta_r,\gamma), \tag{12}$$

where Y_f, Y_r mean the cornering force acting on the front wheels and the real wheels (Figure 7).

In four-wheel vehicle dynamics, the steering of two front wheels is quite important input to the yaw rate. In a wheelchair dynamics, however, the front wheels consist of casters and are not fixed so that the heading angle of the front wheels can be identified with the direction of the wheelchair's moving velocity, V in Figure 7. This means β_f in the front wheels is quite small and there will be little cornering force in the front wheels. This is the most different point of a wheelchair dynamics from that of a four-wheel vehicle.

There is a research which analyzes the effect of this β_f in a wheelchair motion [6]. It illustrates the effects of β_f based on experiments, and the effect proves to be transient since the ground reaction force caused by the β_f is transient. Based on these facts, this β_f is assumed to be zero in this paper, and consequently the cornering forces Y_f, Y_r are given as the following.

$$Y_f = -K_f\beta_f \quad = \quad 0 \tag{13}$$

$$Y_r = -K_r\beta_r \quad = \quad -K_r\left(\beta - l_r\frac{\gamma}{V}\right) \tag{14}$$

Based on this consideration, the transfer function from the gravity to the rotated angle $\alpha = \int \gamma dt$ which we want to estimate, is given as a second order system. However, we try to approximate it to a first order time delay system.

$$\frac{\gamma}{g_{\text{lat}}} = \frac{\dot{\alpha}}{g_{\text{lat}}} = \frac{K}{s^2+2\zeta\omega_n s+\omega_n^2} \rightarrow \frac{K}{s+\omega_o} \tag{15}$$

In this approximation, the error in the phase is the biggest problem. However, the gravity does not change so fast that this approximation in the high frequency region will not cause estimation error. This simplification results in the following dynamics

equations.

$$\ddot{x}_l = -\frac{D}{M}\dot{x}_l + \frac{1}{M}(u_f - R_x - Mg\sin\alpha\sin\xi) \tag{16}$$

$$\ddot{\alpha} = -\frac{B}{I}\dot{\alpha} + \frac{1}{I}(u_\tau - Mgl_r\cos\alpha\sin\xi), \tag{17}$$

where M is the weight of a user and a wheelchair, R_x is the rolling resistance in the longitudinal direction. Rolling resistance in the yaw direction is quite small and it is assumed zero.

These motion equations are verified by comparison of simulation results and experimental result. A wheelchair is located on a slope as the Figure 2. The gravity affects on a wheelchair laterally and the heading angle changes by the gravity. Figure 8 shows the yaw-rate of the wheelchair in the experiments and the simulation.

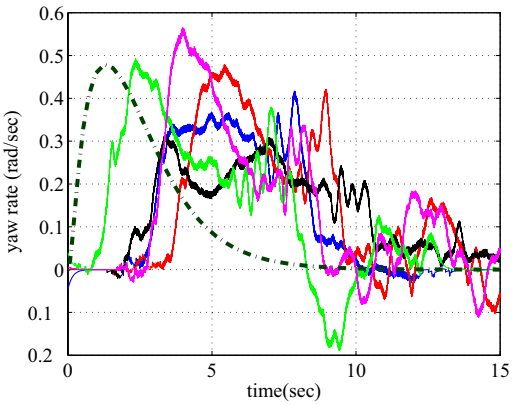

Figure 8. Comparison of Yaw-rates in Experiments and Simulation

Dotted line is the simulation result. This line shows the same motion with the other five experimental results which are described as five solid lines. The oscillations in the experimental results are caused by rough terrain after the downward slope. The changes in the beginning are quite similar, which demonstrates that our modeling of dynamics is right.

This modeling and sensor output analysis leads to the states definition which is shown in Equation (18).

$$\begin{aligned} x &= \begin{pmatrix} x_l & \alpha & \dot{x}_l & \dot{\alpha} & \xi & \dot{\xi} \end{pmatrix}^T \\ &= \begin{pmatrix} x_1 & x_2 & x_3 & x_4 & x_5 & x_6 \end{pmatrix}^T \end{aligned} \tag{18}$$

x_5 is terrain condition which means the slope of a hill, x_2 is the heading angle of a wheelchair and also can be terrain condition, and x_3 is the velocity which is necessary for various power assist control of a wheelchair [7].

$$\begin{aligned} \dot{x} &= \begin{pmatrix} x_3 \\ x_4 \\ -\frac{D}{M}x_3 - g\sin x_2\sin x_5 \\ -\frac{B}{I}x_4 - \frac{M}{I}g\cos x_2\sin x_5 \\ x_6 \\ 0 \end{pmatrix} + \begin{pmatrix} 0 \\ 0 \\ \frac{1}{M}u_f \\ \frac{1}{I}u_\tau \\ 0 \\ 0 \end{pmatrix} \\ &= f(x) + g(u) \end{aligned} \tag{19}$$

$$\begin{aligned} y &= \begin{pmatrix} x_1 \\ x_2 \\ x_4\cos x_2\sin x_5 + x_6\sin x_2\cos x_5 \\ \dot{x}_3 + g\sin x_2\sin x_5 + m_{acc}d_{accx}x_4^2 \\ Mx_3x_4 + g\cos x_2\sin x_5 + m_{acc}d_{accy}x_4^2 \\ g\cos x_5 \end{pmatrix} \\ &= \begin{pmatrix} x_1 \\ x_2 \\ x_4\cos x_2\sin x_5 + x_6\sin x_2\cos x_5 \\ -\frac{D}{M}x_3 + m_{acc}d_{accx}x_4^2 + \frac{1}{M}u_f \\ Mx_3x_4 + g\cos x_2\sin x_5 + m_{acc}d_{accy}x_4^2 \\ g\cos x_5 \end{pmatrix} \\ &= h(x,u) \end{aligned} \tag{20}$$

Notice that we include $\dot{\xi}$ as a state. Changes in ξ or the slope angle are random and difficult to model. If we include this change as a disturbance state, it will simplify the model. This idea will be verified in simulations in Section 4.

3 Design of Nonlinear Operational States Observer for a Wheelchair

With the equations derived in last section, an operation states observer is designed in this section.

3.1 Extension of Kalman Filter to Nonlinear Region

Since the dynamics and sensor outputs have nonlinear characteristics, the extended kalman filter (EKF) algorithm is adopted in this research. This EKF is an effective method to estimate the states of nonlinear dynamics in Equation (21) and (22) [8].

$$x(t) = f(x(t-1)) + g(u(t-1),x) + w(t), \tag{21}$$

$$y(t) = h(x(t)) + e(t), \tag{22}$$

where $w(t)$ and $e(t)$ are white noise sequences which have zero mean and covariance matrix Q and R respectively.

Based on these model equations, the two procedures of Kalman filter, the prediction and the update are given as

$$\bar{x}(t) = f(x(t-1)) + g(u(t-1)) \quad (23)$$
$$\hat{y}(t) = h(\bar{x}(t)) \quad (24)$$
$$\hat{x}(t) = \bar{x}(t) + K(t)(y(t) - \hat{y}(t)) \quad (25)$$

The problem is the decision of the gain $K(t)$ which will optimize the covariance of estimation error under a certain system and measurement noises. As the optimization of the gain $K(t)$ in linear systems is done calculating the transition of error covariance matrix, the linearized transition equation in nonlinear systems also can conduct the same optimization. From this viewpoint, linearization approximation becomes necessary.

Since the Taylor expansion can work as this linearization, three matrixes in Equation (26) to (28) will linearize the nonlinear system.

$$F(t) = \left.\frac{\partial f(t,x)}{\partial x}\right|_{x=\hat{x}(t)} \quad (26)$$
$$G(t) = g(x)|_{x=\hat{x}(t)} \quad (27)$$
$$H(t) = \left.\frac{\partial h(t,x)}{\partial x}\right|_{x=\bar{x}(t)} \quad (28)$$

With these matrixes, the estimation error covariance matrix $P(t+1|t)$ and the gain $K(t)$ will be given as

$$K(t) = P(t|t-1)H^T(t)\left(H(t)P(t|t-1)H^T(t)+R\right)^{-1} \quad (29)$$
$$P(t|t) = P(t|t-1) - K(t)H(t)P(t|t-1) \quad (30)$$
$$P(t+1|t) = F(t)P(t|t)F^T(t) + G(t)V(t)G^T(t), \quad (31)$$

where R and V are the covariance matrixes of the white noise $w(t)$ and $e(t)$ in Equation (21) and (22).

We should notice that since the gain $K(t)$ is derived from the approximation, it is likely to estimate the states correctly but is not an optimal one. To overcome this incorrectness, other observer designs such as the unscented filter [9] are proposed.

3.2 Application of Extended Kalman Filter to a Wheelchair

In order to apply this EKF design to our observer, three matrixes $F(t), G(t)$ and $H(t)$ should be derived from the equation (19) and (20). Equation (32) and (33) represents the derived linearized matrixes.

With these matrixes, an extended operation states observer for a wheelchair is designed. In the next section, we will verify our design using simulations.

4 Simulation Results

Main purposes of simulations conducted in this section are two: one is the verification of observer design, which means it will be checked whether the extended operation states observer can correctly estimate the states in spite of the linearization approximation done in EKF design. The other is the verification of how effect it is to introduce ξ and $\dot{\xi}$ as states.

Three cases are simulated: 1) a wheelchair goes up a hill perpendicular to the horizon, 2) a wheelchair goes up a hill not perpendicular to the horizon, 3) a wheelchair attempts to change its heading angle on a hill.

At first, when a wheelchair climbs a hill perpendicular to the horizon, the gravity affects only the moving velocity and the state α will keep its value as $\frac{\pi}{2}$.

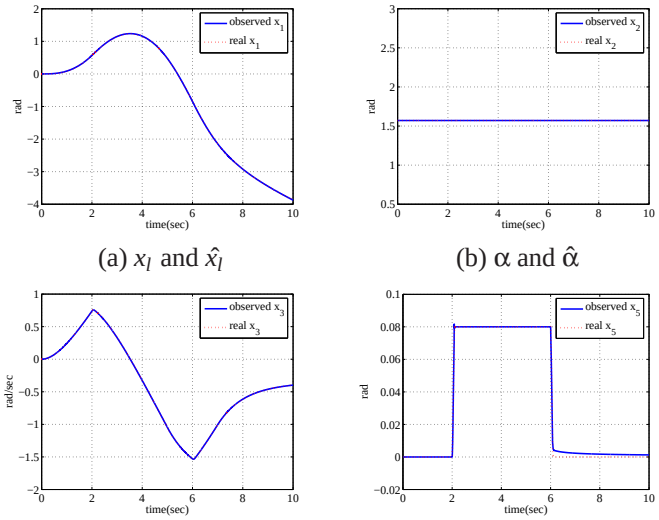

(a) x_l and $\hat{x}_l$ (b) α and $\hat{\alpha}$

(c) $\dot{x}_l$ and $\hat{\dot{x}}_l$ (d) ξ and $\hat{\xi}$

Figure 9. Simulation 1) Perpendicular Climbing

Figure 9 shows the result of this perpendicular climbing simulation. Changes in ξ means a wheelchair goes up a hill of 0.08 rad from 2 to 6 second. Since torque to propel a wheelchair in the longitudinal direction is applied to a wheelchair (the pattern of torque is illustrated in Figure 10 (f)), it starts to move and the state x_l increases for the moment. However, after the wheelchair goes up a hill x_l and $\dot{x}_l$ start to decrease. This is simulated in the result, and we can check that the proposed observer correctly estimates the states.

Figure 10 is the simulation result when a wheelchair goes up a hill with α $\frac{\pi}{3}$. If the heading angle is not perpendicular to the horizon, the gravity affects the heading angle and makes the wheelchair turn. This motions is well simulated and we can see in Figure (b) that α moves to $-\frac{\pi}{2}$ due to the gravity. The proposed

$$F(t) = \begin{pmatrix} 0 & 0 & 1 & 0 & 0 & 0 \\ 0 & 0 & 0 & 1 & 0 & 0 \\ 0 & -g\cos x_2 \sin x_5 & -\frac{D}{M} & 0 & -g\sin x_2 \cos x_5 & 0 \\ 0 & \frac{M}{I} g \sin x_2 \sin x_5 & 0 & -\frac{B}{I} & -\frac{M}{I} g \cos x_2 \cos x_5 & 0 \\ 0 & 0 & 0 & 0 & 0 & 1 \\ 0 & 0 & 0 & 0 & 0 & 0 \end{pmatrix} \tag{32}$$

$$H(t) = \begin{pmatrix} 1 & 0 & 0 & 0 & 0 & 0 \\ 0 & 1 & 0 & 0 & 0 & 0 \\ 0 & -x_4 \sin x_2 \sin x_5 + x_6 \cos x_2 \cos x_5 & 0 & \cos x_2 \sin x_5 & x_4 \cos x_2 \cos x_5 - x_6 \sin x_2 \sin x_5 & \sin x_2 \cos x_5 \\ 0 & 0 & -\frac{D}{M} & 2m_{\mathrm{acc}} d_{\mathrm{accx}} x_4 & 0 & 0 \\ 0 & -g \sin x_2 \sin x_5 & Mx_4 Mx_3 + 2m_{\mathrm{acc}} d_{\mathrm{accxy}} x_4 & & g \cos x_2 \cos x_5 & 0 \\ 0 & 0 & 0 & 0 & -g \sin x_5 & 0 \\ 0 & 0 & 0 & 0 & 0 & 0 \end{pmatrix} \tag{33}$$

observer can correctly estimate the states also in this case. However, $\hat{\xi}$, the observed slope angle is somewhat incorrect. Since the state ξ does not have any model and is only handled as a disturbance, these incorrectness cannot be avoided.

Figure 11 is the simulation results of a wheelchair on which a user attempts to change the heading angle at 1.5 and 6.5 seconds. Figure (f) shows the yaw moment applied by a user.

Around 1.5 second, α starts to increase from $\frac{\pi}{2}$ by the yaw moment. After 2 second, the gravity starts to affect α since it is not perpendicular to the horizon. α increases due to the gravity from 2 to 6 second. After 6 second, the wheelchair is on level ground again and α is only driven by the applied yaw moment.

In this case, the simulation results show that the proposed observer also estimate the states correctly.

5 Conclusion

In this paper, an extended operation states observer is proposed. It can estimate the heading angle of a wheelchair and the slope angle on which the wheelchair is as well as wheelchair's moving velocity.

Simplified motion equations of a wheelchair in the longitudinal and lateral directions are derived and utilized in the design of the observer. Considering the nonlinear characteristics of these motions, the Extended Kalman Filter design is adopted. Simulation results verify this observer correctly estimates all states in various operational environments.

Experimental results in this paper demonstrate that our derivation of the dynamics model and sensor output model is right. The verification by simulations certifies the EKF algorithm is right.

The one point which is not cleared in this paper is the robustness of the proposed observer. Since the dynamics model in Equation (32) and (33) has some parameters which can vary during operation such as the distance between the center of gravity and acceleration, and the weight of the whole wheelchair system, estimation based on that model can be wrong.

Sensors used in this research themselves can be a solution to this robust problem. Since the states estimated by the observer can also be calculated algebraically from the sensor outputs, the model in Equation (32) and (33) plays additional role in estimation and thus errors in parameter values will not cause so much estimation error. In addition to this robustness resulting from enough sensors, states which absorb modeling errors

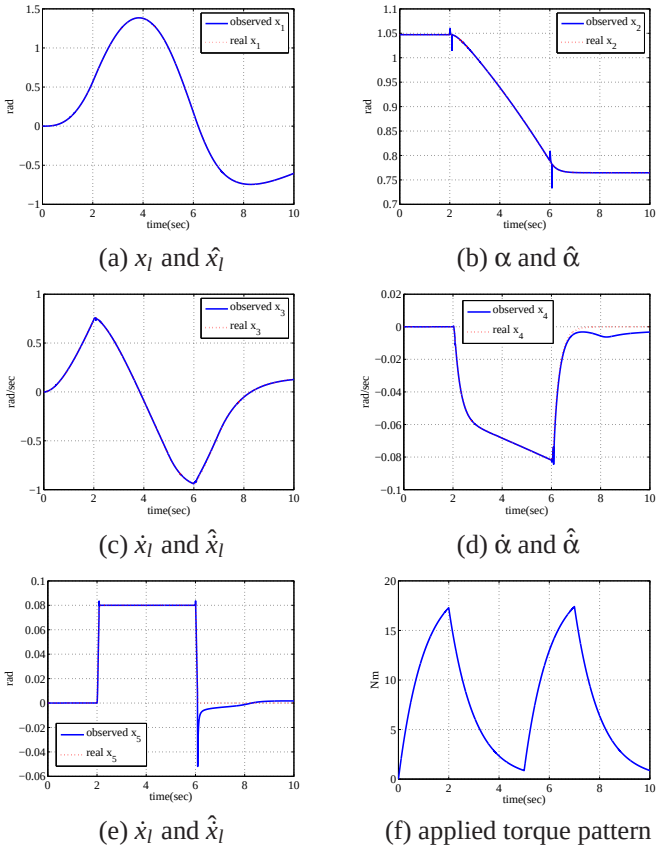

(a) x_l and $\hat{x_l}$ (b) α and $\hat{\alpha}$

(c) $\dot{x_l}$ and $\hat{\dot{x}_l}$ (d) $\dot{\alpha}$ and $\hat{\dot{\alpha}}$

(e) $\dot{x_l}$ and $\hat{\dot{x}_l}$ (f) applied torque pattern

Figure 10. Simulation 2) Climbing with the heading angle $\frac{\pi}{3}$

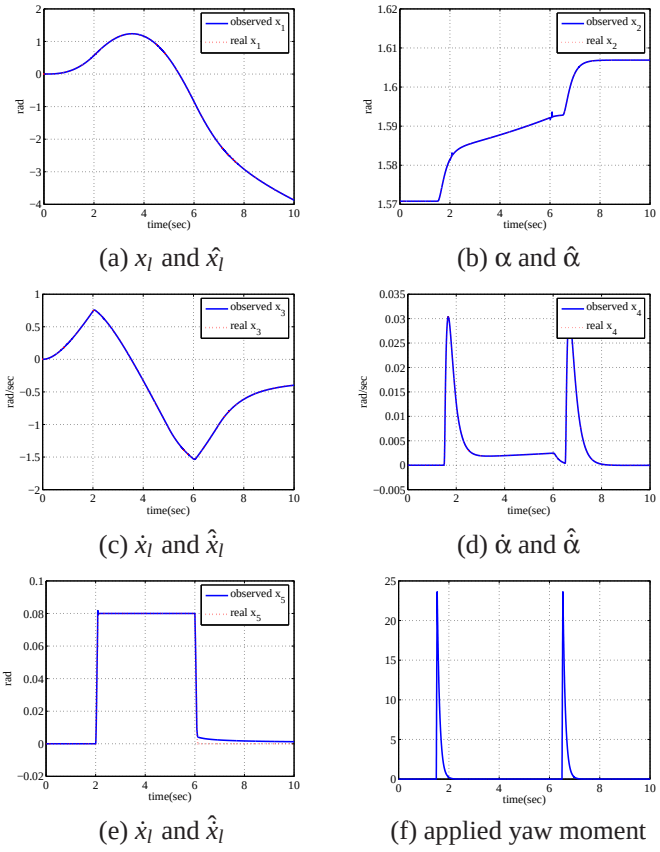

(a) x_l and $\hat{x_l}$ (b) α and $\hat{\alpha}$

(c) $\dot{x_l}$ and $\hat{\dot{x}_l}$ (d) $\dot{\alpha}$ and $\hat{\dot{\alpha}}$

(e) $\dot{x_l}$ and $\hat{\dot{x}_l}$ (f) applied yaw moment

Figure 11. Simulation 3) Attempts to Change α

can be added to improve robustness. Our previous observer [3] has the disturbance states and that could simplify and robustify dynamics model.

The effectiveness of the proposed observer and the idea of robustness should be implemented to a wheelchair and experimented. This is our future works.

REFERENCES

[1] Cooper, R.A.,1995. "Intelligent Control of Power Wheelchairs" *Engineering in Medicine and Biology Magazine, IEEE*, **14** (4), July-Aug, pp.423 - 431

[2] Cooper, R.A., Fitzgerald, S.G., Boninger, M.L., Prins, K.., Rentschler, A.J., Arva, J., O'connor, T.J.,2001. "Evaluation of a Pushrim-Activated, Power-Assisted Wheelchair". *Archives of Physical Medicine and Rehabilitation*, **82**(5), May, pp.702-8

[3] Oh, S., Hata, N. and Hori, Y., 2005. "Control Developments for Wheelchairs in Slope Environments" *American Control Conference*, pp. 739-744.

[4] Luca C., Alessandro D.L., Stefano I., 1999. "Trajectory Tracking Control of a Four-Wheel Differentially Driven Mobile Robot",*Proceedings of the IEEE International Conference on Robotics & Automation*, **5**, pp. 2632-2638.

[5] Guy C., Georges B., and Brigitte D.N., 1996. "Structual Properties and Classificaiton of Kinematic and Dynamic Models of Wheeled Mobile Robots", *IEEE Trans. on Robotics and Automation*, **12**(1), pp. 47-62

[6] Ding D., Cooper R.A. , Guo S., and Corfman T.A., 2004. "Analysis of Driving Backward in an Electric-Powered Wheelchair", *IEEE Trans. on Control Systems Technology*, **12**(6), pp. 934-943

[7] Oh, S., Hata, N., Hori, Y., 2006. "Integrated Motion Control of a Wheelchair in the Longitudinal, Lateral and Pitch Directions" *Proceedings of 9th IEEE International Workshop on Advanced Motion Control*, March,**3**, pp.2214- 2219

[8] T. Söderström, 2002. *Discrete-time Stochastic Systems*.

[9] Simon J.J. and Jeffrey K.U., 2004. "Unscented Filtering and Nonlinear Estimation," *Proceedings of the IEEE*, ,**92**(3), pp. 401-422.